

# Homogeneous Time Constants Promote Oscillations in Negative Feedback Loops

Franco Blanchini,<sup>†</sup> Christian Cuba Samaniego,<sup>‡</sup> Elisa Franco,<sup>‡,§</sup> and Giulia Giordano<sup>\*,§</sup>

<sup>†</sup>Dipartimento di Scienze Matematiche, Informatiche e Fisiche, Università degli Studi di Udine, 33100 Udine, Italy

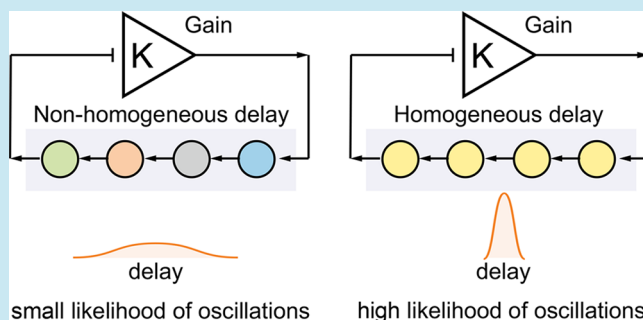
<sup>‡</sup>Department of Mechanical Engineering, University of California at Riverside, Riverside, California 92521, United States

<sup>§</sup>Delft Center for Systems and Control, Delft University of Technology, 2628 CD Delft, The Netherlands

## Supporting Information

**ABSTRACT:** Biological oscillators are present in nearly all self-regulating systems, from individual cells to entire organisms. In any oscillator structure, a negative feedback loop is necessary, but not sufficient to guarantee the emergence of periodic behaviors. The likelihood of oscillations can be improved by careful tuning of the system time constants and by increasing the loop gain, yet it is unclear whether there is any general relationship between optimal time constants and loop gain. This issue is particularly relevant in genetic oscillators resulting from a chain of different subsequent biochemical events, each with distinct (and uncertain) kinetics. Using two families of genetic oscillators as model examples, we show that the loop gain required for oscillations is minimum when all elements in the loop have the same time constant. On the contrary, we show that homeostasis is ensured if a single element is considerably slower than the others.

**KEYWORDS:** oscillations, delays, time constants, feedback, biomolecular oscillators, synthetic biology



Timekeeping elements coordinate and synchronize most processes required to sustain life, from the physiology of individual cells to the daily rhythms of entire organisms.<sup>1</sup> The design principles underlying the operation of biomolecular clocks have been investigated by dissecting natural systems,<sup>2–5</sup> as well as by building *de novo* molecular oscillators in an effort to identify minimal requirements for periodic behaviors.<sup>6–10</sup> Experiments<sup>6,2,7,9,11</sup> and modeling<sup>12–21</sup> have established that a necessary requirement for a system to exhibit oscillations is the presence of a negative loop. Conversely, any negative feedback loop potentially leads to oscillations provided that the loop includes destabilizing features, for instance delaying elements associated with a large feedback gain.<sup>7,22,23</sup> Delay can be introduced by a variety of phenomena. In addition to transcription and translation steps, delay is increased by transport, mRNA splicing and stabilization, phosphorylation, and protein maturation.<sup>24,25,46</sup> While an explicit delay term is useful to aggregate these phenomena in a single, black-box parameter, in other instances it is possible to model their individual kinetics as a chain of interconnected subsystems.<sup>17,25,26</sup> In a linearized closed-loop system, a chain of slow subsystems has the same effects as an explicit delay in inducing oscillations.<sup>22</sup> The overall delay of the negative feedback chain depends on all the time constants of the dynamic elements. Given a sufficient delay, the larger the feedback gain, the likelier is the onset of persistent oscillations.

Despite the simplicity of these design principles, it is unclear how the individual time constants and the overall gain affect the

emergence of oscillations. Are we equally likely to observe oscillations in a system with homogeneous *versus* nonhomogeneous time scales? How large should the loop gain be in either case? These questions are particularly relevant in the context of genetic oscillators, where time constants are determined by mRNA and protein degradation, transport, and processing rates, which may widely vary among the oscillator components, and a large loop gain is energetically expensive, because it depends on the production rate of the components.

In this paper, we address the following question in mathematical terms: Given a negative loop of first order elements, each associated with its own time constant, which is the choice of the time constants that requires the smallest gain to allow for persistent oscillations? We demonstrate that homogeneous time constants are the most favorable choice when a small loop gain is desired. In particular we prove that (1) the smallest negative feedback gain required to trigger oscillations is achieved when all time constant are equal; (2) the smallest gain is invariant under a homogeneous scaling of all time constants and the period of the oscillations is proportional to the scaling factor; (3) as a converse result, in a negative feedback loop, the best strategy to avoid oscillations is to have a single element of the chain that is much slower than all the others, and this fact explains why, in several pathways with

**Received:** December 6, 2017

**Published:** April 20, 2018

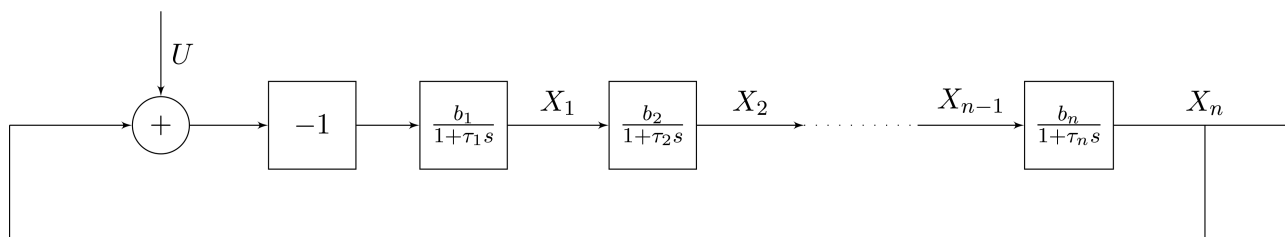


Figure 1. Loop of  $n$  first order systems: block diagram.

negative feedback, the presence of a slow element ensures a robust nonoscillatory behavior.

We apply our results to well-known genetic oscillators, the Goodwin oscillator and a two-node (inhibitor-activator) oscillator, and we derive exact (necessary and sufficient) conditions for the existence of parameters that ensure oscillations.

**Architecture of Candidate Negative Feedback Oscillators.** As candidate oscillator architectures, we consider negative feedback loops of the following form:

$$\begin{aligned} \tau_1 \dot{x}_1(t) &= -x_1(t) - b_1[x_n(t) + u(t)] \\ \tau_i \dot{x}_i(t) &= -x_i(t) + b_i x_{i-1}(t), \quad i = 2, \dots, n \end{aligned} \quad (1)$$

representing the series connections of  $n$  ordered subsystems in which any element has a positive influence, quantified by parameters  $b_i > 0$  (with  $i = 2, \dots, n$ ), on the next one, while  $u$  is a perturbing input that triggers oscillations. Each ordinary differential equation (ODE) in the model in eq 1 is suited to model phenomena such as production, conversion, processing, and degradation of molecular components (mRNA and proteins) interconnected in a regulatory chain.<sup>27</sup> The model can also capture enzymatic processes that operate at low substrate concentration relative to the binding affinity of the enzyme and substrate; in this regime, Michaelian or Hill-type reaction rates become approximately linear (first-order rates). A negative feedback loop is generated *via* the inhibitory effect of the last element in the chain on the first one, quantified by parameter  $b_1 > 0$ . The parameter  $\tau_i$  represents the time constant of process  $i$  (which can be seen as the speed of the reaction of the species  $x_i$  due to the regulatory effect of  $x_{i-1}$ ).

A similar negative feedback structure can be found in many oscillatory systems.<sup>17</sup> We now take the Laplace transform of these ODEs: we formally replace  $x_i(t)$  with  $X_i(s)$  and the derivative  $d/dt$  with the complex variable  $s$ ,  $\dot{x}_i(t) \rightarrow sX_i(s)$ . After Laplace-transformation, the model in eq 1 can be rewritten as a block-interconnection of elements:

$$\begin{aligned} X_1 &= \frac{-b_1}{1 + \tau_1 s} (X_n + U), & X_i &= \frac{b_i}{1 + \tau_i s} X_{i-1}, \\ & & i &= 2, \dots, n \end{aligned}$$

as shown in Figure 1.

The quantity

$$\kappa \doteq \prod_{i=1}^n b_i > 0$$

is called the *loop gain* and has a fundamental role. It is the product of all the interaction strengths and thus represents the cumulative strength of the loop. It turns out that the characteristic polynomial depends on the product  $\kappa$  only, and not on the individual parameters  $b_i$ ; hence, even if the individual

rates  $b_i$  are changed, the system behavior remains the same as long as their product is unchanged (see the Supporting Information for the detailed derivation). The onset of oscillations in this negative feedback loop is therefore associated with two fundamental ingredients:

- The time constants  $\tau_i$ , which introduce an overall *delay* in the loop;
- A sufficiently large feedback gain  $\kappa > 0$ .

In the next section we ask ourselves whether there is any ideal relationship between the loop gain and the time constants to achieve or avoid oscillatory behavior.

**Influence of Time Constants on the Oscillatory Regime.** We next investigate how the time constants  $\tau_i$  influence the onset of persistent oscillations. We define  $\tau = [\tau_1 \ \tau_2 \ \dots \ \tau_n]$ , the vector of time constants, and consider the characteristic polynomial associated with the (linearized) system of ODEs:

$$\begin{aligned} p_n(s, \tau) &= \kappa + (1 + \tau_1 s)(1 + \tau_2 s) \dots (1 + \tau_n s) \\ &= \kappa + \prod_{i=1}^n (1 + \tau_i s) \end{aligned} \quad (2)$$

For  $\kappa = 0$ , the roots of  $p_n(s, \tau)$  are  $\lambda_i = -1/\tau_i$ , real and negative, hence the system response has an exponentially decreasing pattern. For large values of  $\kappa$ ,  $p_n(s, \tau)$  has complex roots, associated with oscillations.

The oscillations are damped if the roots have a negative real part. To have persistent oscillations, the roots of  $p_n(s, \tau)$  must reach and cross the imaginary axis in the complex plane. This can happen only if

$$n \geq 3$$

(as discussed at the end of this section; see also ref 28). Henceforth, we assume that the necessary condition  $n \geq 3$  is verified.

For  $n \geq 3$ , let us increase  $\kappa$ . Then, there exists a *critical gain*  $\kappa^*$  such that, for all  $\kappa > \kappa^*$ ,  $p_n(s, \tau)$  has complex roots with positive real part (namely, the system becomes unstable). For  $\kappa = \kappa^*$ ,  $p_n(s, \tau)$  has two purely imaginary roots  $\pm j\omega^*$ , while the other roots have negative real part. The limit value  $\kappa^*$  is associated with the onset of an oscillation with frequency  $\omega^*/2\pi$ ; we call  $\omega^*$  *critical pulsation*. Note that  $\omega^* \neq 0$ :  $p_n(s, \tau)$  cannot have 0 as a root for  $\kappa > 0$ , since  $p(0, \tau) = \kappa + 1 \neq 0$ .

We can formally define the critical gain  $\kappa^*$  as the smallest value of  $\kappa$  for which  $p_n(s, \tau)$  has a pair of purely imaginary roots (corresponding to the stability limit). The value  $\kappa^*$  depends on the time constants  $\tau_i$  and we can write

$$\kappa^*(\tau) = \min\{\kappa > 0: p_n(j\omega, \tau) = 0 \text{ for some } \omega > 0\} \quad (3)$$

Which are the most favorable values of  $\tau_i$  to promote oscillations? We address this question in terms of the *minimum*

critical gain, by seeking a value  $\tau^* = [\tau_1^* \tau_2^* \dots \tau_n^*]$  that minimizes the critical  $\kappa^*(\tau)$  enabling the onset of oscillations.

**Problem:** Find a value  $\tau^*$  that minimizes  $\kappa^*(\tau)$  in eq 3.

**Main result:** The problem is solved by a value  $\tau^*$  with

$$\tau_1^* = \tau_2^* = \dots = \tau_n^*$$

This result is proved in the [Supporting Information](#) (Theorem 1): our proofs are based on frequency analysis tools, linear algebraic tools and principles of convex optimization.

Therefore, an essential factor to promote oscillations in a negative feedback loop is the homogeneity of the time constants of the subsystems involved in the loop.

Further, we find that scaling the time constants influences exclusively the critical pulsation, without affecting the critical gain: when the time constants are scaled as  $\tau_i \rightarrow \sigma\tau_i$ , for arbitrary  $\sigma > 0$ , the critical gain  $\kappa^*$  is invariant,  $\kappa^*(\sigma\tau^*) = \kappa^*(\tau^*)$ , while the critical pulsation scales proportionally to  $\sigma$ :  $\omega^* \rightarrow \sigma\omega^*$  (cf. Corollary 1, [Supporting Information](#)).

Also, the critical gain  $\kappa^*$  is a decreasing function of the number of elements in the loop (see the [Supporting Information](#), Proposition 2, for details).

Our result (the critical gain that allows for oscillations is minimized when all the time constants are equal) indirectly suggests how to prevent a system from oscillating. This aspect is relevant in the context of biological and biochemical feedback loops, in all the situations where it is important to preserve homeostasis and oscillatory behaviors must be avoided. Being  $\kappa^*$  a decreasing function of  $n$ , long feedback chains are more prone to instability, which can be of an oscillatory type. Hence, a natural question is which is the best strategy to avoid oscillations in the loop. Our result suggests that incongruous time constants lead to a robustly nonoscillatory behavior. Let us now consider the complementary question: assuming (without restriction) that the time constants are normalized as

$$\sum \tau_i = T_{\text{tot}}$$

where  $T_{\text{tot}}$  is the overall loop delay, which is the best distribution of time constants to prevent oscillatory behaviors? We find that, roughly speaking, it is better to have the delay concentrated in a single subsystem (see the [Supporting Information](#), Proposition 3, for details). Then, a robust strategy to prevent oscillations is, for instance, including in the loop a single subsystem that is much slower than the others, so that their time constant is negligible with respect to the slow part. This result also explains the previous statement about the necessity of condition  $n \geq 3$  to have persistent oscillations. Indeed, setting  $\tau_i = 0$  is mathematically equivalent to neglecting the  $i$ th process, since then  $1/(1 + \tau_i s) = 1$ .

A fundamental consequence of our results is the following: in a negative feedback loop, the presence of a single slow element is an effective strategy to preserve stability and prevent oscillations. Indeed, several negative feedback loops in nature are practically always stable, and this can be explained by noting that the involved time constants are very different. For example, biologically, degradation rates of mRNA and proteins may vary in a broad range and, as foreseen by our results, this variability could contribute to stabilizing negative loops, making it difficult to achieve oscillations. Yet, we point out that, when the kinetics of a molecular species are much slower or much faster than the rest of the system, they can be simply eliminated from the model via time scale separation methods;<sup>27</sup> this type of

drastic time scale variability may affect the capacity for oscillations when the system dimension collapses below 3.

**Examples.** Our results allow us to derive analytical bounds in the parameter space for the oscillatory regions of general families of genetic oscillators. These bounds are also numerically verified in the following sections via random parameter sampling.<sup>29</sup>

**Goodwin Oscillator.** The well-known Goodwin oscillator<sup>30</sup> is associated with the following equations:

$$\dot{x}_1 = a_1 \frac{K^N}{K^N + x_n^N} - b_1 x_1 \quad (4)$$

$$\dot{x}_i = a_i x_{i-1} - b_i x_i, \quad i = 2, \dots, n \quad (5)$$

The model is characterized by the number  $n$  of stages, by the cooperativity (Hill) coefficient  $N$ , by the apparent dissociation constant  $K$ , and by the rate constants  $a_i$  and  $b_i$ . Rates  $a_i$  and  $b_i$  can model protein translation and degradation, mRNA processing phenomena, or protein phosphorylation/dephosphorylation.<sup>31</sup> All these parameters are positive. As shown in the [Supporting Information](#) (Section 2.1), the system admits a single positive equilibrium. The emergence of sustained oscillations depends on the choice of the parameters, which influences the values of both the variables at steady-state and of the entries of the Jacobian matrix. By applying our main result to the Goodwin oscillator model, we discover that there exists at least one choice of the parameter values that leads to oscillations (namely, for which the linearized system admits complex eigenvalues with nonnegative real part) if and only if

$$\cos(\pi/n) \sqrt[n]{N} > 1 \quad (6)$$

(the full derivation is in the [Supporting Information](#), Section 2.3). The characteristic equation, equating the characteristic polynomial to zero, is

$$\prod_{i=1}^n (1 + s/b_i) + N \frac{\bar{x}_n^N}{K^N + \bar{x}_n^N} = 0 \quad (7)$$

Here,  $\bar{x}_n$  is the steady state value of  $x_n$  derived by solving the equilibrium equation

$$\frac{K^N}{K^N + x_n^N} = \frac{b_1 b_2 \dots b_n}{a_1 a_2 \dots a_n} x_n = y \quad (8)$$

from which existence and uniqueness of the equilibrium are proven in the [Supporting Information](#) (Section 3.1). If we could arbitrarily choose the rates  $a_i$  and  $b_i$ , then we could achieve any positive steady-state  $\bar{x}_n$ . Hence, the gain in eq 7,

$$\kappa(\bar{x}_n) = N \frac{\bar{x}_n^N}{K^N + \bar{x}_n^N}$$

could take any value in the interval:  $0 < \kappa(\bar{x}_n) < N$ . The value of the  $i$ th time constant for this system is  $\tau_i = 1/b_i$ . Hence, our result tells us that the (minimum) critical gain is obtained by setting  $b_1 = b_2 = \dots = b_n = b$  (which leads to equal time constants), hence

$$(1 + s/b)^n + \kappa(\bar{x}_n) = 0, \quad 0 < \kappa < N \quad (9)$$

The condition in eq 6 is necessary and sufficient for eq 9 to admit imaginary solutions. As exemplified in Figure 2, if the condition in eq 6 is satisfied, oscillations are possible if the rates  $a_i$  are large enough with respect to the rates  $b_i$ ; this guarantees a

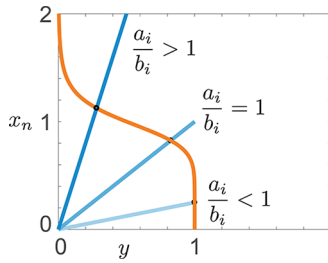


**Figure 2.** Goodwin oscillator: equilibrium conditions for different ratios  $a_i/b_i$ . The orange line represents the first expression in eq 8, while the blue lines represent the second expression in eq 8 for different values of the ratios  $a_i/b_i$ . Their intersections give, on the vertical axis, the equilibrium values of  $x_n$  for various choices of  $a_i/b_i$ .

large equilibrium value  $\bar{x}_n$ , hence  $\kappa(\bar{x}_n)$  is larger than the critical gain.

Note that, if the oscillator includes three stages ( $n = 3$ ), the condition in eq 6 becomes  $\sqrt[3]{N} > 2$  and the minimum value of the Hill coefficient  $N$  to have oscillations is  $N = 8$ , consistently with the results in ref 32.

In Figure 3 we numerically compute the oscillatory region in the  $N$ - $n$  space when  $a_i = a$  and  $b_i = b$ , for all  $i$ . In each panel, the

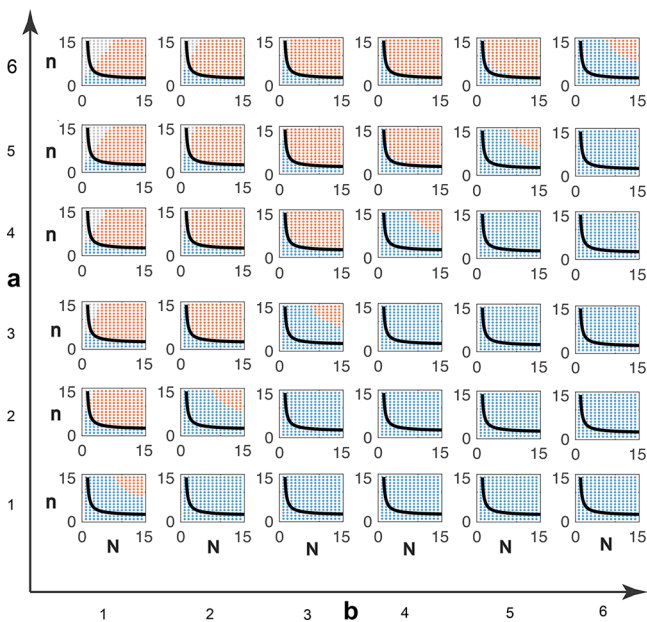


**Figure 3.** Oscillatory domain of the Goodwin oscillator with  $K = 1$  in the  $(n, N)$  plane, for various choices of homogeneous rates,  $a_i = a$  and  $b_i = b$  for all  $i$ . The black line represents  $\cos(\pi/n)\sqrt[3]{N} = 1$ ; hence, eq 6 is satisfied in the whole region above. We compute the solutions of eq 9: red dots indicate an oscillatory behavior, blue dots indicate no oscillations, while gray dots indicate that no equilibrium can be found computationally due to numerical problems.

black line represents the condition in eq 6 converted to an equality, and delimits the region where oscillations can occur. As a further numerical experiment, we fixed  $a_i = a$  for all  $i$  and randomly generated different values of the parameters  $b_i$ , taken from different distributions (normal and uniform distribution) with the same expected value  $E[b_i] = 1$  and variance  $\epsilon$ . With this sampling method, the total delay is not necessarily constant for all samples: the degradation rates are randomly generated and are drawn from different distributions, which all have the same

average, but which can be more or less spread depending on the value of the variance  $\epsilon$ . The lower the variance, the more homogeneous are the degradation rates  $b_i$ . Figure 4 shows the

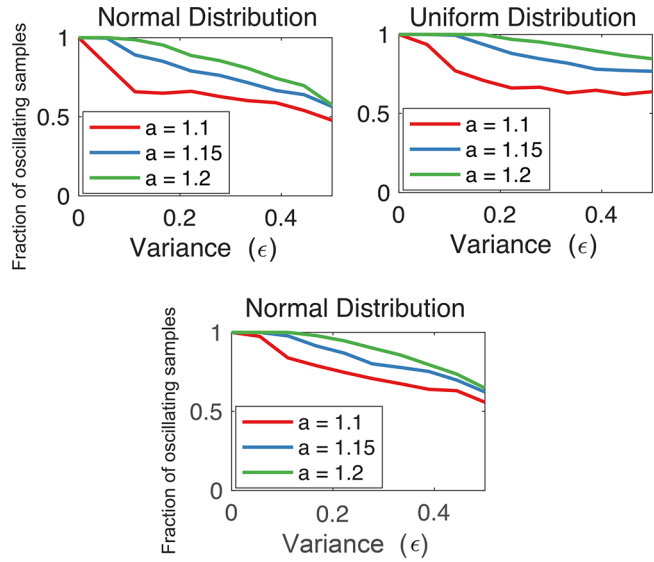


**Figure 4.** The fraction of oscillating samples of the Goodwin oscillator is largest when randomly drawn degradation rates are homogeneous. We simulated the model with  $K = 1$  and  $n = 5$ ; in the top panels  $N = 8$ , while in the bottom panel  $N = 10$ . We took  $a_i = a$  and randomly generated rates  $b_i$  with expected value  $E[b_i] = 1$  and variance  $\epsilon$ . (In each simulation, the randomly generated parameters are kept constant during all the integration steps of the ODEs.) We show the fraction of oscillating samples as a function of the variance  $\epsilon$  when the rates  $b_i$  are taken from a normal distribution (top left, and bottom) and a uniform distribution (top right). In all panels, 1000 parameter samples are drawn per data point.

fraction of oscillating samples (parameter choices for which characteristic polynomial has positive-real-part roots) as a function of  $\epsilon$ . As predicted by our analytical results, decreasing the variance increases the likelihood of oscillations. Choosing homogeneous time constants favors oscillations, but also other design decisions are important: for instance, the overall loop gain needs to be high enough.

**A Two-Node Oscillator.** Consider a two-node oscillator given by the feedback interconnection of an activated module and an inhibited module:<sup>9,33–35</sup>

$$\dot{r}_1 = \frac{\alpha_1}{K_1^N + p_2^N} - \beta_1 r_1 \tag{10}$$

$$\dot{p}_1 = \gamma_1 r_1 - \delta_1 p_1 \tag{11}$$

$$\dot{r}_2 = \frac{\alpha_2 p_1^N}{K_2^N + p_1^N} - \beta_2 r_2 \tag{12}$$

$$\dot{p}_2 = \gamma_2 r_2 - \delta_2 p_2 \tag{13}$$

The ODEs of variables  $r_1$  and  $r_2$  represent mRNA dynamics, and  $p_1, p_2$  represent protein translation. As earlier,  $N$  is a Hill coefficient, and  $K_1$  and  $K_2$  are apparent dissociation constants. Parameters  $\alpha_1$  and  $\alpha_2$  are maximal mRNA transcription rates, and  $\beta_1, \beta_2$  are mRNA degradation rates. Finally  $\gamma_1, \gamma_2$  and  $\delta_1, \delta_2$  are protein translation and degradation rates. This model can serve as a coarse-grained representation of a variety of molecular

clocks. Many genetic oscillators result from the interconnected dynamics of inhibitor-activator elements,<sup>25</sup> such as the p53-mdm-2<sup>36</sup> and the  $\kappa\text{B}$ -NF- $\kappa\text{B}$ <sup>37</sup> oscillators; this architecture has also been demonstrated in artificial *in vitro* transcriptional oscillators.<sup>9,38,39</sup> Here we assume that the mRNA dynamics evolve on a time scale that is comparable to that of the proteins; this means that the order of the model cannot be reduced *via* time scale separation arguments. On the basis of our main result, we can prove that there exists at least one choice of parameters for which the system exhibits sustained oscillations (namely, the linearized system has complex eigenvalues with a nonnegative real part) if and only if

$$N > 2 \quad (14)$$

The linearized system has characteristic equation

$$\left(1 + \frac{s}{\beta_1}\right)\left(1 + \frac{s}{\beta_2}\right)\left(1 + \frac{s}{\delta_1}\right)\left(1 + \frac{s}{\delta_2}\right) + N^2 \frac{K_2^N}{K_2^N + \bar{p}_1^N} \frac{p_2^N}{K_1^N + \bar{p}_2^N} = 0 \quad (15)$$

where  $\bar{p}_1$  and  $\bar{p}_2$  are the steady-state values of  $p_1$  and  $p_2$ . The loop gain

$$\kappa(\bar{p}_1, \bar{p}_2) = N^2 \frac{K_2^N}{K_2^N + \bar{p}_1^N} \frac{p_2^N}{K_1^N + \bar{p}_2^N}$$

ranges in the interval  $0 < \kappa(\bar{p}_1, \bar{p}_2) < N^2$ ; it is a decreasing function of  $\bar{p}_1$ , and an increasing function of  $\bar{p}_2$ . In view of our main result, the minimum critical gain guaranteeing oscillations is achieved when  $\beta_1 = \beta_2 = \delta_1 = \delta_2 = \tau$ . The corresponding critical equation is

$$(1 + s/\tau)^4 + \kappa(\bar{p}_1, \bar{p}_2) = 0, \quad 0 < \kappa(\bar{p}_1, \bar{p}_2) < N^2$$

therefore no unstable complex eigenvalues, hence no oscillations, can be found unless  $N > 2$  (the full derivation is in the [Supporting Information](#), Section 3.3). Numerical simulations illustrating and confirming this analytical result are in [Figure 5](#). We have also generated random instances of the

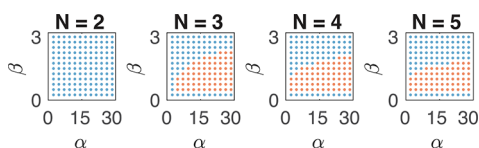


**Figure 5.** Oscillatory regime of the two-node oscillator. We compute the solutions of eq 15, with  $\alpha_1 = \alpha_2 = \alpha$ ,  $\beta_1 = \beta_2 = \beta$ ,  $\gamma_1 = \gamma_2 = 1$ ,  $\delta_1 = \delta_2 = 1$  and  $K_1 = K_2 = 1$ , and indicate with red dots an oscillatory behavior, with blue dots no oscillations. Parameter sets that give rise to oscillations cannot be found for  $N = 2$ , while they are easy to find for  $N > 2$ .

oscillator to show how increasing the variance in the delay decreases the chances of oscillatory behavior ([Figure 6](#)). We note that in this particular example, if the mRNA dynamics are much faster than the protein dynamics, the model can be reduced to include exclusively the protein kinetics; in that case, oscillations cannot be achieved for any choice of the parameters.

**Conclusion and Discussion.** We have demonstrated that homogeneity of the time constants within a negative feedback loop can facilitate the emergence of oscillations, in that it minimizes the critical loop gain (minimum gain to achieve

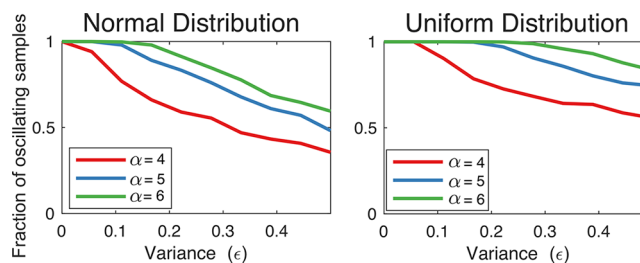


**Figure 6.** The fraction of oscillating samples of the two-node oscillator is largest when randomly drawn degradation rates are homogeneous. We simulated the model with  $N = 3$ ,  $\gamma_1 = \gamma_2 = 1$ ,  $K_1 = K_2 = 1$ ,  $\alpha_1 = \alpha_2 = \alpha$  and randomly generated  $(\beta_i, \delta_i)$  with expected value  $E[(\beta_i, \delta_i)] = (1, 1)$  and variance  $\epsilon$ . (In each simulation, the randomly generated parameters are kept constant during all the integration steps of the ODEs.) We show the fraction of oscillating samples as a function of the variance  $\epsilon$  when  $(\beta_i, \delta_i)$  are taken from a normal distribution (left) and a uniform distribution (right). 1000 parameter samples are drawn per data point.

oscillations). We have also shown that scaling of the (uniform) time constants influences the critical frequency, but does not affect the critical gain. A converse result is that a candidate oscillator can be stabilized, *i.e.*, oscillations cannot occur, by increasing a single (arbitrarily chosen) time constant of the loop with respect to the others. The negative feedback architecture we consider is general, and it can be specialized to model many biomolecular oscillators.<sup>25</sup>

The gain of the biomolecular feedback loops we consider is proportional to the ratio of production and degradation rates of its components, and to the cooperativity coefficient of regulatory molecules (Hill coefficient  $N$ ). Maintaining the lowest gain that can yield oscillations in the network is therefore tantamount to operating the circuit with minimum consumption of transcription and translation resources, minimum kinase activity, as well as with minimum copy number of regulators. This energy-efficient scenario can be achieved when the time constants in each process are similar (degradation, transport, and processing rates). This requirement may be easy to satisfy if these time constants are globally regulated for all components (for instance, mRNA and protein degradation).

It must be pointed out that, in our analysis, we have considered systems consisting of a *single negative feedback loop*: although this is a very common structure for biological oscillators,<sup>17,25</sup> it is not the only one. For this particular structure, we have argued that

- Short negative loops have a stabilizing effect (which makes the onset of sustained oscillations less likely, because a higher loop gain is needed);
- Long negative loops can favor the onset of sustained oscillations, and the most favorable case is that in which the time constants of the system in the loop are similar;
- If one or two time constants are significantly larger than the others, then the long loop actually behaves as a short one and the probability of having sustained oscillations is smaller (because a higher loop gain is needed for the onset of oscillations).

However, if several feedback loops are concurrently present, our analysis does not apply, and the above statements are no longer true. In particular, our findings are valid in the absence of self-catalytic reactions (*i.e.*, of positive self-loops). In the presence of a positive self-loop, also a single negative loop involving two nodes only can be easily destabilized. For instance, consider the system

$$\dot{x}_1 = -ax_1 - bx_2$$

$$\dot{x}_2 = cx_1 - dx_2$$

where  $a$ ,  $b$ ,  $c$  and  $d$  are positive parameters. As shown by our results, this loop cannot be destabilized. However, this system can exhibit sustained oscillations if  $a$  can be negative (take for instance  $a = -d$ ): in this case our results no longer hold, because now  $x_1$  is self-catalytic.

In practice, positive self-loops are not very common. Yet, a positive feedback loop can result from a chain of reactions. Indeed, different oscillator architectures are based on the coexistence of positive and negative loops (it is important to stress that the presence of a negative loop is necessary for the onset of oscillations<sup>14,15</sup>). In particular

- A (possibly short) negative loop can be destabilized by the concurrent presence of another loop that is positive.

An example is the genetic network present in the bread mold *Neurospora crassa*, which has been shown in ref 40 to be a successful biological oscillator; we investigate this case study in the Supporting Information, where we show that the result proposed in ref 40 are fully consistent with our analysis.

Negative-feedback oscillators are very common in nature and appear also very robust. For instance, the Hes1 and Hes7 oscillators in mammalian embryos consist of a negative autoregulation loop where Hes protein represses its mRNA production.<sup>41</sup> These oscillators could be modeled taking  $n = 2$  in eq 1; however, in this case the ODE solution does not admit sustained oscillations even for very large values of  $N$ . Addition of an explicit delay, discrete or distributed, to Hes autoregulatory models yields oscillatory solutions for physically acceptable values of  $N$ <sup>42,43</sup> (Hes1 and Hes7 are dimers). Similar observations can be made for the p53-mdm-2 and the I $\kappa$ B-NF- $\kappa$ B oscillators.<sup>44</sup> The explicit delay, which captures mRNA processing and transport steps,<sup>45</sup> could be alternatively modeled as a chain of intermediate subsystems; while the number and kinetics of these steps are unknown, our results suggest that oscillations would be more likely to occur if they had similar time scales. Interestingly, the Hes1 oscillator requires nearly identical mRNA and protein half-lives ( $\approx 23$  min) to operate.<sup>46</sup>

Our results are particularly relevant for the design of artificial negative feedback clocks. While the architecture of the Goodwin oscillator is attractive due to its simplicity, it has been difficult to build synthetic examples without including positive feedback, high Hill coefficients, or additional nonlinearities to destabilize the system.<sup>6,7,16,47</sup> The mathematical models developed to capture the dynamics of these artificial oscillators often assume similar degradation rates for all the mRNA and protein species. However, recent experiments on the famous *repressilator* circuit suggest that protein degradation rates in the original design might have been subject to temporal fluctuations caused by competition for shared proteolytic machinery, occurring due to the presence of protein degradation tags meant to reduce their half-life.<sup>48</sup> Removal of the degradation tags resulted in more regular (although slower) oscillations at the population level. It is possible that in the absence of degradation tags dilution (due to cells dividing) becomes the dominant time constant, which should be uniform for all the repressor proteins. In light of our results, a more homogeneous protein half-life could explain the improved robustness of the oscillations.

In conclusion, our work highlights that the variability of time constants within negative feedback oscillators could have underappreciated effects on the dynamics; better estimation of these

parameters could help explain the robustness of many natural oscillators. Conversely, we expect that the construction or improvement of artificial oscillators could be facilitated by ensuring that the modules being interconnected evolve with similar time scales.

## METHODS

The formal proofs of our results, which employ mathematical tools from dynamical systems and systems and control theory, as well as the detailed mathematical analysis of the proposed examples, are in the Supporting Information.

## ASSOCIATED CONTENT

### Supporting Information

The Supporting Information is available free of charge on the ACS Publications website at DOI: 10.1021/acssynbio.7b00442.

Proofs of our theoretical results; Detailed analysis of the Goodwin oscillator; Detailed analysis of a two-node oscillator; Case study: the *Neurospora crassa* biological clock (PDF)

## AUTHOR INFORMATION

### Corresponding Author

\*E-mail: g.giordano@tudelft.nl.

### ORCID

Elisa Franco: 0000-0003-1103-2668

Giulia Giordano: 0000-0002-8600-1738

### Author Contributions

F.B., E.F. and G.G. conceived, designed and performed the research; F.B. and G.G. contributed the mathematical analysis, results and derivations; E.F. contributed the biological contextualisation and interpretation; C.C.S. performed the numerical experiments and simulations; all the authors wrote the manuscript and participated in its revision.

### Notes

The authors declare no competing financial interest.

## ACKNOWLEDGMENTS

This work was supported by the National Science Foundation under Grant CMMI-1266402 and by the Aspasia Grant (3mE Faculty) at the Delft University of Technology.

## REFERENCES

- (1) Harrisingh, M. C., and Nitabach, M. N. (2008) Integrating circadian timekeeping with cellular physiology. *Science* 320 (5878), 879–880.
- (2) Pomerening, J. R., Sontag, E. D., and Ferrell, J. E. (2003) Building a cell cycle oscillator: hysteresis and bistability in the activation of Cdc2. *Nat. Cell Biol.* 5 (4), 346–351.
- (3) Nakajima, M., Imai, K., Ito, H., Nishiwaki, T., Murayama, Y., Iwasaki, H., et al. (2005) Reconstitution of Circadian Oscillation of Cyanobacterial KaiC Phosphorylation in Vitro. *Science* 308 (5720), 414–415.
- (4) O'Neill, J. S., Maywood, E. S., Chesham, J. E., Takahashi, J. S., and Hastings, M. H. (2008) cAMP-dependent signaling as a core component of the mammalian circadian pacemaker. *Science* 320 (5878), 949–953.
- (5) Pokhilko, A., Fernandez, A. P., Edwards, K. D., Southern, M. M., Halliday, K. J., and Millar, A. J. (2012) The clock gene circuit in *Arabidopsis* includes a repressilator with additional feedback loops. *Mol. Syst. Biol.* 8, 574.
- (6) Elowitz, M. B., and Leibler, S. (2000) A synthetic oscillatory network of transcriptional regulators. *Nature* 403 (6767), 335–338.

- (7) Stricker, J., Cookson, S., Bennett, M. R., Mather, W. H., Tsimring, L. S., and Hasty, J. (2008) A fast, robust and tunable synthetic gene oscillator. *Nature* 456 (7221), 516–519.
- (8) Tigges, M., Dénervaud, N., Greber, D., Stelling, J., and Fussenegger, M. (2010) A synthetic low-frequency mammalian oscillator. *Nucleic Acids Res.* 38 (8), 2702–2711.
- (9) Kim, J., and Winfree, E. (2011) Synthetic *in vitro* transcriptional oscillators. *Mol. Syst. Biol.* 7, 465.
- (10) Semenov, S. N., Wong, A. S., Van Der Made, R. M., Postma, S. G., Groen, J., Van Roekel, H. W., et al. (2015) Rational design of functional and tunable oscillating enzymatic networks. *Nat. Chem.* 7 (2), 160–165.
- (11) Montagne, K., Plasson, R., Sakai, Y., Fujii, T., and Rondelez, Y. (2011) Programming an *in vitro* DNA oscillator using a molecular networking strategy. *Mol. Syst. Biol.* 7, 466.
- (12) Thomas, R. (1981) On the relation between the logical structure of systems and their ability to generate multiple steady states or sustained oscillations, in *Numerical Methods in the Study of Critical Phenomena* (Della-Dora, J., Demongeot, J., and Lacolle, B., Ed.), Vol. 9, Springer-Verlag.
- (13) Luo, Y., and Epstein, I. R. (1990) in *Feedback Analysis of Mechanisms for Chemical Oscillators*, pp 269–299, John Wiley & Sons, Inc.
- (14) Gouze, J. L. (1998) Positive and Negative Circuits in Dynamical Systems. *J. Biol. Syst.* 6, 11–15.
- (15) Snoussi, E. H. (1998) Necessary conditions for multistationarity and stable periodicity. *J. Biol. Syst.* 6, 3–9.
- (16) Tsai, T. Y. C., Choi, Y. S., Ma, W., Pomerening, J. R., Tang, C., and Ferrell, J. E. J. (2008) Robust, Tunable Biological Oscillations from Interlinked Positive and Negative Feedback Loops. *Science* 321 (5885), 126–129.
- (17) Novak, B., and Tyson, J. J. (2008) Design principles of biochemical oscillators. *Nat. Rev. Mol. Cell Biol.* 9 (12), 981–991.
- (18) Angeli, D., and Sontag, E. D. (2008) Oscillations in I/O monotone systems. *IEEE Trans. Autom. Control* 55, 166–176.
- (19) Domijan, M., and Kirkilionis, M. (2009) Bistability and oscillations in chemical reaction networks. *J. Math Biol.* 59, 4.
- (20) Blanchini, F., Franco, E., and Giordano, G. (2014) A Structural Classification of Candidate Oscillatory and Multistationary Biochemical Systems. *Bull. Math. Biol.* 76 (10), 2542–2569.
- (21) Blanchini, F., Franco, E., and Giordano, G. (2015) Structural conditions for oscillations and multistationarity in aggregate monotone systems, in *IEEE 54th Annual Conference on Decision and Control (CDC)*, pp 609–614, Osaka, Japan.
- (22) Rapp, P. (1976) Analysis Of Biochemical Phase-Shift Oscillators By A Harmonic Balancing Technique. *J. Math Biol.* 3, 203–224.
- (23) Hori, Y., and Hara, S. (2011) Time delay effects on oscillation profiles in cyclic gene regulatory networks: Harmonic balance approach. *Proc. Am. Control Conf.*, 2891–2896.
- (24) Ruoff, P., Vinsjevsk, M., Monnerjahn, C., and Rensing, L. (1999) The Goodwin oscillator: on the importance of degradation reactions in the circadian clock. *J. Biol. Rhythms* 14 (6), 469–479.
- (25) Tiana, G., Krishna, S., Pigolotti, S., Jensen, M. H., and Sneppen, K. (2007) Oscillations and temporal signalling in cells. *Phys. Biol.* 4 (2), R1.
- (26) Mengel, B., Hunziker, A., Pedersen, L., Trusina, A., Jensen, M. H., and Krishna, S. (2010) Modeling oscillatory control in NF- $\kappa$ B, p53 and Wnt signaling. *Curr. Opin. Genet. Dev.* 20 (6), 656–664.
- (27) Alon, U. (2006) *An Introduction to Systems Biology: Design Principles of Biological Circuits*, Chapman & Hall/CRC.
- (28) Kurosawa, G., Mochizuki, A., and Iwasa, Y. (2002) Comparative study of circadian clock models, in search of processes promoting oscillation. *J. Theor. Biol.* 216 (2), 193–208.
- (29) Mattingly, H. H., Sheintuch, M., and Shvartsman, S. Y. (2017) The Design Space of the Embryonic Cell Cycle Oscillator. *Biophys. J.* 113 (3), 743–752.
- (30) Goodwin, B. C. (1965) Oscillatory behavior in enzymatic control processes. *Adv. Enzyme Regul.* 3, 425–438.
- (31) Heinrich, R., Neel, B. G., and Rapoport, T. A. (2002) Mathematical models of protein kinase signal transduction. *Mol. Cell* 9 (5), 957–970.
- (32) Griffith, J. (1968) Mathematics of cellular control processes I. Negative feedback to one gene. *J. Theor. Biol.* 20 (2), 202–208.
- (33) Blanchini, F., Cuba Samaniego, C., Franco, E., and Giordano, G. (2014) Design of a molecular clock with RNA-mediated regulation, in *IEEE 53rd Annual Conference on Decision and Control (CDC)*, pp 4611–4616, Los Angeles, California.
- (34) Cuba Samaniego, C., Giordano, G., Kim, J., Blanchini, F., and Franco, E. (2016) Molecular titration promotes oscillations and bistability in minimal network models with monomeric regulators. *ACS Synth. Biol.* 5, 321–333.
- (35) Cuba Samaniego, C., Giordano, G., Blanchini, F., and Franco, E. (2017) Stability analysis of an artificial biomolecular oscillator with non-cooperative regulatory interactions. *J. Biol. Dynamics* 11 (1), 102–120.
- (36) Wu, X., Bayle, J. H., Olson, D., and Levine, A. J. (1993) The p53-mdm-2 autoregulatory feedback loop. *Genes Dev.* 7 (7a), 1126–1132.
- (37) Hoffmann, A., Levchenko, A., Scott, M. L., and Baltimore, D. (2002) The I $\kappa$ B-NF- $\kappa$ B signaling module: temporal control and selective gene activation. *Science* 298 (5596), 1241–1245.
- (38) Franco, E., Friedrichs, E., Kim, J., Jungmann, R., Murray, R., Winfree, E., et al. (2011) Timing molecular motion and production with a synthetic transcriptional clock. *Proc. Natl. Acad. Sci. U. S. A.* 108 (40), E784–E793.
- (39) Weitz, M., Kim, J., Kapsner, K., Winfree, E., Franco, E., and Simmel, F. C. (2014) Diversity in the dynamical behaviour of a compartmentalized programmable biochemical oscillator. *Nat. Chem.* 6 (4), 295–302.
- (40) Yu, Y., Dong, W., Altimus, C., Tang, X., Griffith, J., Morello, M., Dudek, L., Arnold, J., and Schüttler, H.-B. (2007) A genetic network for the clock of *Neurospora crassa*. *Proc. Natl. Acad. Sci. U. S. A.* 104 (8), 2809–2814.
- (41) Kageyama, R., Ohtsuka, T., and Kobayashi, T. (2007) The Hes gene family: repressors and oscillators that orchestrate embryogenesis. *Development* 134 (7), 1243–1251.
- (42) Jensen, M., Sneppen, K., and Tiana, G. (2003) Sustained oscillations and time delays in gene expression of protein Hes1. *FEBS Lett.* 541 (1–3), 176–177.
- (43) Rateitschak, K., and Wolkenhauer, O. (2007) Intracellular delay limits cyclic changes in gene expression. *Math. Biosci.* 205 (2), 163–179.
- (44) Monk, N. A. (2003) Oscillatory expression of Hes1, p53, and NF- $\kappa$ B driven by transcriptional time delays. *Curr. Biol.* 13 (16), 1409–1413.
- (45) Takashima, Y., Ohtsuka, T., González, A., Miyachi, H., and Kageyama, R. (2011) Intronic delay is essential for oscillatory expression in the segmentation clock. *Proc. Natl. Acad. Sci. U. S. A.* 108 (8), 3300–3305.
- (46) Hirata, H., Yoshiura, S., Ohtsuka, T., Bessho, Y., Harada, T., Yoshikawa, K., et al. (2002) Oscillatory expression of the bHLH factor Hes1 regulated by a negative feedback loop. *Science* 298 (5594), 840–843.
- (47) Danino, T., Mondragon-Palmino, O., Tsimring, L., and Hasty, J. (2010) A synchronized quorum of genetic clocks. *Nature* 463 (7279), 326–330.
- (48) Potvin-Trottier, L., Lord, N. D., Vinnicombe, G., and Paulsson, J. (2016) Synchronous long-term oscillations in a synthetic gene circuit. *Nature* 538 (7626), 514–517.

# Homogeneous time constants promote oscillations in negative feedback loops

---

## Supplementary Material

---

Franco Blanchini<sup>1</sup>, Christian Cuba Samaniego<sup>2</sup>, Elisa Franco<sup>3</sup>, and Giulia Giordano<sup>4,\*</sup>

<sup>1</sup>*Dipartimento di Matematica, Informatica e Fisica, Università degli Studi di Udine, 33100 Udine, Italy.*

<sup>2</sup>*Department of Mechanical Engineering, University of California at Riverside, 900 University Avenue, Riverside, CA 92521, USA.*

<sup>3</sup>*Department of Mechanical Engineering, University of California at Riverside, 900 University Avenue, Riverside, CA 92521, USA.*

<sup>4</sup>*Delft Center for Systems and Control, Delft University of Technology, Mekelweg 2, 2628 CD Delft, The Netherlands.*

*\*Corresponding author, g.giordano@tudelft.nl.*

# Contents

<b>1</b>	<b>Proofs of the theoretical results</b>	<b>3</b>
<b>2</b>	<b>Analysis of the Goodwin oscillator</b>	<b>6</b>
2.1	Goodwin oscillator: model and equilibrium . . . . .	6
2.2	Goodwin oscillator: linearisation . . . . .	6
2.3	Goodwin oscillator: conditions for sustained oscillations . . . . .	8
<b>3</b>	<b>Analysis of a two-node oscillator</b>	<b>9</b>
3.1	Two-node oscillator: model and equilibrium . . . . .	9
3.2	Two-node oscillator: linearisation . . . . .	10
3.3	Two-node oscillator: conditions for sustained oscillations . . . . .	11
<b>4</b>	<b>A case study: the Neurospora crassa biological clock</b>	<b>12</b>

# 1 Proofs of the theoretical results

The negative feedback interconnection of  $n \in \mathbb{N}$  first order systems (cf. Fig. 1 of the Main Paper, where  $n \geq 3$ ) can be represented in the Laplace domain as

$$\begin{aligned} X_n(s) &= -\frac{b_1}{1 + \tau_1 s} \frac{b_2}{1 + \tau_2 s} \cdots \frac{b_n}{1 + \tau_n s} [X_n(s) + U(s)] \\ &= -\kappa \prod_{i=1}^n \left( \frac{1}{1 + \tau_i s} \right) [X_n(s) + U(s)], \end{aligned}$$

where  $\kappa \doteq \prod_{i=1}^n b_i > 0$  is the loop gain, as defined in the main paper, and  $\tau_i > 0$  for all  $i$ , hence  $\tau = [\tau_1 \ \tau_2 \ \dots \ \tau_n]$  is a positive vector in  $\mathbb{R}^n$ . The transfer function from  $U(s)$  to  $X_n(s)$  is

$$F(s) = \frac{-\kappa}{\kappa + \prod_{i=1}^n (1 + \tau_i s)}.$$

Hence the characteristic polynomial associated with the loop, which corresponds to the denominator of the above transfer function, is

$$p_n(s, \tau) = \kappa + \prod_{i=1}^n (1 + \tau_i s)$$

and depends on the product  $\kappa \doteq \prod_{i=1}^n b_i$ , but not on the individual values of the parameters  $b_i$ . For  $n > 2$  and large  $\kappa > 0$ ,  $p_n(s, \tau)$  has positive-real-part roots, associated with instability phenomena. When  $\kappa = \kappa^*$ , the *critical gain*,  $p_n(s, \tau)$  has a pair of purely imaginary roots.

In the Main Paper, we aim at solving the following problem.

**Problem 1** Find a value  $\tau^*$  that minimises the critical gain  $\kappa^*(\tau)$ , namely that minimises

$$\kappa^*(\tau) = \min\{\kappa > 0 : p_n(j\omega, \tau) = 0 \text{ for some } \omega > 0\}.$$

Our main result is summarised in the following theorem.

**Theorem 1** Problem 1 is solved by a value  $\tau^*$  with

$$\tau_1^* = \tau_2^* = \dots = \tau_n^*.$$

Hence,  $\kappa^*(\tau^*) = \min_{\tau > 0} \kappa^*(\tau)$ .

We give here the proof of Theorem 1, which also requires an intermediate proposition and a corollary.

**Proof of Theorem 1.**

The minimum destabilising gain as a function of  $\tau$  can be denoted as

$$\kappa^*(\tau) = \min\{\kappa : \exists \omega \text{ such that } p_n(j\omega, \tau) = 0\}.$$

For a given  $\tau$ ,  $\kappa^*(\tau)$  is the smallest value of  $\kappa$  such that the characteristic polynomial  $p_n(j\omega, \tau)$  is not Hurwitz (i.e., does not have all negative-real-part roots) and necessarily admits a pair of complex, purely imaginary, roots. To proceed with our proof, we state the following proposition, showing that  $\kappa^*(\sigma\tau)$  is constant with respect to  $\sigma$ ; namely, even when  $\tau$  is scaled, the polynomial  $p_n$  admits a pair of imaginary roots for the same value of  $\kappa = \kappa^*$ .

**Proposition 1** For any  $\sigma > 0$ ,  $\kappa^*(\sigma\tau) = \kappa^*(\tau)$ .

**Proof of Proposition 1:** For a given  $\tau \in \mathbb{R}^n$ , if  $p_n(s, \tau)$  has a pair of imaginary roots  $s = \pm j\omega$ , then  $p_n(s, \sigma\tau)$  has roots scaled as  $s = \pm j\omega/\sigma$ . Indeed,  $\kappa + \prod_{i=1}^n (1 + \tau_i j\omega) = 0$  for some  $\omega$  if and only if

$$\kappa + \prod_{i=1}^n (1 + (\sigma\tau_i)j\frac{\omega}{\sigma}) = \kappa + \prod_{i=1}^n (1 + (\sigma\tau_i)j\omega') = 0$$

for some  $\omega' = \omega/\sigma$ . ■

We have thus proved that  $\kappa^*(\sigma\tau)$  is invariant with respect to  $\sigma > 0$ , while the pulsation of the oscillations  $\omega$  changes as  $\omega' = \omega/\sigma$ .

**Corollary 1** When the time constants are scaled as  $\tau_i \rightarrow \sigma\tau_i$ , for arbitrary  $\sigma > 0$ , the critical gain  $\kappa^*$  is invariant,  $\kappa^*(\sigma\tau^*) = \kappa^*(\tau^*)$ , while the critical pulsation scales proportionally to  $\sigma$ :  $\omega^* \rightarrow \sigma\omega^*$ .

Then, the solution of the problem is time-scale invariant: we can equivalently consider the problem in which the critical frequency is scaled to  $\omega = 1$ , namely, minimise  $\kappa$  such that  $p_n(j, \tau) = 0$ :

$$\min_{\tau > 0} \kappa > 0 \tag{1}$$

$$\text{s.t. } \kappa + \prod_{i=1}^n (1 + j\tau_i) = 0 \tag{2}$$

The complex expression (2) corresponds to two real constraints. Let us parameterise the numbers  $(1 + j\tau_i)$  as follows:

$$(1 + j\tau_i) = \sqrt{1 + \tau_i^2} e^{j\arctan(\tau_i)}, \quad i = 1, \dots, n.$$

Now, (2) can be rewritten as  $\prod_{i=1}^n (1 + j\tau_i) = -\kappa$ , where  $-\kappa$  is negative real. Then, the problem in (1) and (2) is equivalent to minimising  $\kappa > 0$  under the conditions

$$\prod_{i=1}^n \sqrt{1 + \tau_i^2} = \kappa, \quad \sum_{i=1}^n \arctan(\tau_i) = m\pi,$$

for  $m > 0$  integer and odd, with  $\tau_i > 0$ . It is not difficult to see that the minimum is achieved for  $m = 1$ : in fact, in order to increase the phase, the  $\tau_i$ 's must be increased, and this increases the modulus  $\kappa$  as well. Then, we can consider the problem

$$\min \prod_{i=1}^n (1 + \tau_i^2) \quad \text{s.t.} \quad \sum_{i=1}^n \arctan(\tau_i) = \pi, \quad \tau_i > 0.$$

This minimisation problem can be recast as a convex optimisation problem by defining the new variable  $\theta_i = \arctan(\tau_i)$ ,  $\theta_i \in (0, \pi/2]$ , and considering the logarithm of the objective function. We obtain

$$\min \sum_{i=1}^n \log[1 + \tan^2(\theta_i)] \tag{3}$$

$$\text{s.t.} \quad \sum_{i=1}^n \theta_i = \pi, \quad \theta_i \in (0, \pi/2], \tag{4}$$

which is a convex problem, since (4) are linear constraints and (3) is a strictly convex function. Indeed, it is the sum of  $n$  strictly convex functions of one variable: for the function  $\log[1 + \tan^2(\theta_i)]$ , the first derivative is  $2 \tan(\theta_i)$ , while the second derivative is  $1/\cos^2(\theta_i)$ , which is always positive. (Alternatively: the objective function as a multivariable function and its Hessian is a diagonal matrix with positive diagonal entries, hence it is positive definite, which implies strict convexity of the function.)

At the minimum, in view of the optimality conditions, the gradient of the objective function (with respect to the variables  $\theta_i$ , i.e.,  $\nabla(\cdot) = \partial(\cdot)/\partial\tau$ ) is aligned with the gradient of the constraint. The method of Lagrange multipliers, with multiplier  $\lambda$ , gives

$$\frac{\partial}{\partial\tau} \left[ \sum_{i=1}^n \log[1 + \tan^2(\theta_i)] \right] = \lambda \frac{\partial}{\partial\tau} \left[ \sum_{i=1}^n \theta_i \right].$$

By equating the two gradients component by component, we get

$$2 \tan(\theta_i) = \lambda, \quad k = 1, 2, \dots, n,$$

which implies that  $\theta_i$  are all equal; since  $\tau_i = \tan(\theta_i)$ , this in turn implies that  $\tau_i$  are all equal,  $\tau_i = \hat{\tau} \forall i$ .

The Lagrange multiplier condition is just necessary for a minimum. However, since the objective function is strictly convex, as previously shown, the stationary point found by the Lagrange multiplier method is indeed a minimum, and the proof is over.

**End of the Proof of Theorem 1.** ■

For all  $i$ ,  $\tau_i^* = \hat{\tau}$ , with  $\hat{\tau} = \tan(\pi/n)$ , since  $n \arctan(\hat{\tau}) = \pi$ , and the optimal value of  $\kappa$  turns out to be  $\kappa^* = [1 + \tan(\pi/n)^2]^{\frac{n}{2}}$ , which is independent of the common value of the time constant  $\hat{\tau}$ .

In the previous computations we have normalised the frequency to  $\omega = 1$  essentially by setting  $(1 + j\omega\tau) = (1 + j\tilde{\tau})$ . To derive the actual critical frequency associated with choosing  $\tau_i = \hat{\tau}$  for all  $i$ , we can see that  $(\omega^*\tau) = \tan(\pi/n)$ , hence  $\omega^* = \frac{\tan(\pi/n)}{\hat{\tau}}$ . As expected,  $\omega^*$  is a decreasing function of  $n$ .

The next two propositions show that the critical gain is a decreasing function of the number of elements in the loop, and that oscillations are prevented if one delay is significantly larger than the others.

**Proposition 2** *Denote by  $\kappa_{n_1}^*$  and  $\kappa_{n_2}^*$  the critical gain values associated with loops involving  $n = n_1$  and  $n = n_2$  elements, respectively. Then, if  $n_1 > n_2$ ,  $\kappa_{n_1}^* < \kappa_{n_2}^*$ .*

**Proof of Proposition 2.** We need to prove that the minimum value  $\kappa^*$  of  $\kappa$ , solution of the considered optimisation problem (3)–(4), is a decreasing function of  $n$ , the number of elements in the loop. If the value of  $\tau$  providing the minimum  $\kappa_{n_1}^*$  (for  $n = n_1$ ) is such that  $\tau_1^* = \tau_2^* = \dots = \tau_{n_1}^*$ , solving the problem with  $n_2 < n_1$  corresponds to solving the previous problem in the restricted domain where, for instance, the first  $r = n_1 - n_2$   $\tau_i$ 's are zero:  $\tau_1 = \dots = \tau_r = 0$ . However, since the objective function is strictly convex and the minimum is internal, as shown in the proof of Theorem 1, a smaller value cannot be achieved on the boundary of the closure of the domain. ■

**Proposition 3** *If  $\tau_1 = T_{tot}$  and  $\tau_i = 0$ ,  $i \geq 2$ , there are no oscillations (not even damped): all the roots of  $p_n(s, \tau)$  are real. If  $\tau_1 + \tau_2 = T_{tot}$  and  $\tau_i = 0$ ,  $i \geq 3$ , there are no permanent oscillations: there are no complex roots of  $p_n(s, \tau)$  with a nonnegative real part.*

**Proof of Proposition 3.** If just  $\tau_1 = T_{tot}$  is nonzero, the loop equation is  $(1 + \tau_1 s) + \kappa = 0$ , whose only root is real and negative; hence, there are no oscillations. If  $\tau_1 + \tau_2 = T_{tot}$ , the equation is  $(1 + \tau_1 s)(1 + \tau_2 s) + \kappa = 0$  and can have two complex roots for  $\kappa$  large; yet their real part is negative: the oscillations are damped. ■

## 2 Analysis of the Goodwin oscillator

We propose in this section a detailed analysis of the well renowned Goodwin oscillator [8]. In our analysis, we exploit Theorem 1, which states that the minimum gain required for the onset of oscillations in a negative feedback loop is minimised when the time constants of the subsystems involved in the loop are homogeneous. The results in Theorem 1 allow us to quantitatively bound the oscillatory domain of the Goodwin oscillator and derive exact oscillatory conditions in the parameter space.

### 2.1 Goodwin oscillator: model and equilibrium

The equations of a Goodwin oscillator [8] with  $n$  stages and Hill coefficient  $N$  are

$$\dot{x}_1 = a_1 \frac{K^N}{K^N + x_n^N} - b_1 x_1 \quad (5)$$

$$\dot{x}_i = a_i x_{i-1} - b_i x_i, \quad i = 2, \dots, n \quad (6)$$

where  $a_i$  and  $b_i$ , for  $i = 1, \dots, n$ , and  $K$  are positive coefficients.

At the equilibrium, we have  $\dot{x}_i = 0$  for all  $i$ . Then, from Eq. (6) at the equilibrium we get

$$\bar{x}_{i-1} = \frac{b_i}{a_i} \bar{x}_i, \quad i = 2, \dots, n, \quad (7)$$

hence we can derive  $\bar{x}_1$  as a function of  $\bar{x}_n$ :

$$\bar{x}_1 = \frac{b_2 b_3 \dots b_n}{a_2 a_3 \dots a_n} \bar{x}_n. \quad (8)$$

From Eq. (5) at the equilibrium we get

$$\bar{x}_1 = \frac{a_1}{b_1} \frac{K^N}{K^N + \bar{x}_n^N}. \quad (9)$$

Then, considering Eq. (8) and Eq. (9) together, we obtain that the equilibrium value  $\bar{x}_n$  is the solution of the following equation:

$$\frac{K^N}{K^N + \bar{x}_n^N} = \frac{b_1 b_2 b_3 \dots b_n}{a_1 a_2 a_3 \dots a_n} \bar{x}_n = y, \quad (10)$$

where the variable  $y$  has been introduced to aid the visualisation in Figure 1. The first expression is a bounded, decreasing function of  $\bar{x}_n$ , the second expression is a linear function of  $\bar{x}_n$  and is a line with positive slope, increasing up to infinity. Hence, there always exists a single positive intersection  $\bar{x}_n > 0$ , as shown in Figure 1. Once  $\bar{x}_n$  has been found, the equilibrium values of all the other variables can be derived recursively, by exploiting the relations in Eq. (7).

### 2.2 Goodwin oscillator: linearisation

The Jacobian matrix associated with the linearisation of the system in Eqs. (5)–(6), around the unique equilibrium point computed in the previous section, is given by

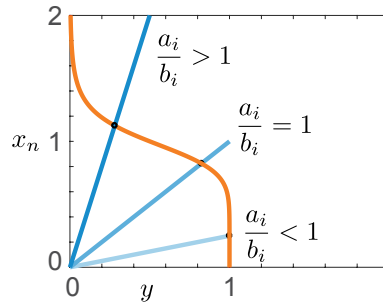


Figure 1: Goodwin oscillator: equilibrium conditions for different ratios  $a_i/b_i$ .

$$J_G = \begin{bmatrix} -b_1 & 0 & 0 & \dots & 0 & \frac{-a_1 N K^N \bar{x}_n^{N-1}}{(K^N + \bar{x}_n^N)^2} \\ a_2 & -b_2 & 0 & \dots & 0 & 0 \\ 0 & a_3 & -b_3 & \dots & 0 & 0 \\ \vdots & \vdots & \vdots & \ddots & \vdots & \vdots \\ 0 & 0 & 0 & \dots & -b_{n-1} & 0 \\ 0 & 0 & 0 & \dots & a_n & -b_n \end{bmatrix}, \quad (11)$$

and corresponds to the characteristic polynomial

$$p_G(s) = \det(sI - J_G) = \prod_{i=1}^n (s + b_i) + \prod_{i=1}^n a_i \frac{N K^N \bar{x}_n^{N-1}}{(K^N + \bar{x}_n^N)^2}.$$

Enforcing the relation derived from (10)

$$\frac{\prod_{i=1}^n a_i K^N}{K^N + \bar{x}_n^N} = \bar{x}_n \prod_{i=1}^n b_i \quad (12)$$

that stems from the equilibrium conditions, the characteristic polynomial becomes

$$p_G(s) = \prod_{i=1}^n (s + b_i) + N \frac{\bar{x}_n^N}{K^N + \bar{x}_n^N} \prod_{i=1}^n b_i.$$

Dividing  $p_G(s)$  by  $\prod_{i=1}^n b_i$ , we can write the characteristic equation as

$$\prod_{i=1}^n (1 + s/b_i) + N \frac{\bar{x}_n^N}{K^N + \bar{x}_n^N} = 0. \quad (13)$$

The dynamic behaviour and the stability properties of the linearised system around the equilibrium point, including its capability of giving rise to persistent oscillations, are ruled by the roots of  $p_G(s)$ , namely, by the solutions of the characteristic equation (13).

**Remark 1** The coefficients  $1/b_i$  correspond to the time constants  $\tau_i$  in Eq. (3) of the Main Paper, while the term  $N \frac{\bar{x}_n^N}{K^N + \bar{x}_n^N}$  corresponds to the gain  $\kappa$  in Eq. (3) of the Main Paper.

### 2.3 Goodwin oscillator: conditions for sustained oscillations

We would like to find the minimum value  $N^*$  of  $N$  for which the system exhibits sustained oscillations, namely, the characteristic equation (13) admits a pair of complex solutions with nonnegative real part (i.e., the linearised system admits a pair of complex eigenvalues with nonnegative real part). In view of the results in Theorem 1, the minimum value  $N^*$  is achieved when all  $b_i$ 's are equal:  $b_i = b^*$  for all  $i$ . Then, the equation we need to solve is

$$(1 + s/b^*)^n + N \frac{\bar{x}_n^N}{K^N + \bar{x}_n^N} = 0,$$

hence

$$\frac{s}{b^*} = -1 + \sqrt[n]{-1} \sqrt[n]{N} \sqrt[n]{\frac{\bar{x}_n^N}{K^N + \bar{x}_n^N}}. \quad (14)$$

Since  $0 < \frac{\bar{x}_n^N}{K^N + \bar{x}_n^N} < 1$ , the critical condition for the characteristic equation (13) to admit complex solutions with a nonnegative real part is:

$$\cos(\pi/n) \sqrt[n]{N} > 1. \quad (15)$$

We can therefore state the following result, which allows us to characterise the subset of the parameter space where oscillations are indeed possible.

**Proposition 4** *The two following conditions are equivalent.*

- (i) *There exists at least one choice of parameters for the Goodwin oscillator for which the characteristic equation (13) admits complex solutions with nonnegative real part.*
- (ii) *The inequality (15) is satisfied.*

**Proof** We first show that (ii) is necessary for (i). Indeed, the smallest value of the gain required to have oscillations is achieved when all the  $b_i$ 's are equal, according to Theorem 1. For  $b_1 = b_2 = \dots = b_n$ , the roots of the characteristic polynomial satisfy Eq. (14). The two roots having the largest real part (i.e., the two *dominant* roots) satisfy

$$\frac{s}{b^*} = -1 + \sqrt[n]{N} e^{\pm j\pi/n} \sqrt[n]{\frac{\bar{x}_n^N}{K^N + \bar{x}_n^N}}.$$

Since  $0 < \frac{\bar{x}_n^N}{K^N + \bar{x}_n^N} < 1$ , their real part

$$\operatorname{Re}\left(\frac{s}{b^*}\right) = -1 + \sqrt[n]{N} \cos(\pi/n) \sqrt[n]{\frac{\bar{x}_n^N}{K^N + \bar{x}_n^N}}$$

can be larger than 0 only if the condition (15) is satisfied.

To prove that (ii) is sufficient for (i), consider again the equilibrium condition in Eq. (12) and write it as

$$\frac{1}{K^N + \bar{x}_n^N} = \frac{b_1 b_2 \dots b_n}{a_1 a_2 \dots a_n} \bar{x}_n.$$

It is not difficult to see that, if we take

$$\frac{b_1 b_2 \dots b_n}{a_1 a_2 \dots a_n} = \frac{b^n}{a_1 a_2 \dots a_n}$$

large, then the root  $\bar{x}_n$  can become arbitrarily large (as is also shown in Figure 1). Hence, we can ensure that, for a suitable choice of the parameters, the fraction

$$\sqrt[n]{\frac{\bar{x}_n^N}{K^N + \bar{x}_n^N}}$$

gets arbitrarily close to 1. Then, if the condition (15) holds, the real part of the two dominant roots can indeed cross the imaginary axis. ■

It is worth pointing out that, in the case of  $n = 3$ , the condition in (15) becomes  $\sqrt[3]{N} > 2$  and the minimum value of  $N$  to have oscillations is  $N = 8$ , consistently with the results in [10]. The general condition that we have derived based on Theorem 1, however, can be applied to Goodwin oscillators with an arbitrary number of stages.

### 3 Analysis of a two-node oscillator

We propose in this section a detailed analysis of a two-node oscillator, resulting from the (overall negative) feedback interconnection of an activated module and an inhibited module [2, 5, 6, 7, 11]. Also in this case, the results in Theorem 1 allow us to precisely characterise the oscillatory domain of the two-node oscillator in the parameter space.

#### 3.1 Two-node oscillator: model and equilibrium

A two-node oscillator is given by the feedback interconnection of an activated module and an inhibited module

$$\dot{r}_1 = \frac{\alpha_1}{K_1^N + p_2^N} - \beta_1 r_1 \tag{16}$$

$$\dot{p}_1 = \gamma_1 r_1 - \delta_1 p_1 \tag{17}$$

$$\dot{r}_2 = \frac{\alpha_2 p_1^N}{K_2^N + p_1^N} - \beta_2 r_2 \tag{18}$$

$$\dot{p}_2 = \gamma_2 r_2 - \delta_2 p_2 \tag{19}$$

where  $\alpha_i, \beta_i, \gamma_i, \delta_i$  and  $K_i$ , for  $i = 1, 2$ , are positive parameters.

At the equilibrium,  $\dot{r}_i = \dot{p}_i = 0$ , for  $i = 1, 2$ . Hence, we can derive the following equilibrium conditions: the equilibrium pair  $(\bar{p}_1, \bar{p}_2)$  is the solution of the coupled equations

$$p_1 = \frac{\alpha_1 \gamma_1}{\beta_1 \delta_1} \frac{1}{K_1^N + p_2^N} \tag{20}$$

$$p_2 = \frac{\alpha_2 \gamma_2}{\beta_2 \delta_2} \frac{p_1^N}{K_2^N + p_1^N}, \tag{21}$$

which always exists and is unique because in Eq. (20) the variable  $p_1$  is expressed as a decreasing function of  $p_2$ , while in Eq. (21) the variable  $p_2$  is expressed as an increasing function of  $p_1$ , hence the two curves always have exactly one intersection. Then, once  $\bar{p}_1$  and  $\bar{p}_2$  have been found, the equilibrium values of the other variables can be computed as

$$\bar{r}_i = \frac{\delta_i}{\gamma_i} \bar{p}_i, \quad i = 1, 2.$$

### 3.2 Two-node oscillator: linearisation

The Jacobian matrix that describes the linearisation of the system in Eqs. (16)–(19) in a neighbourhood of the equilibrium point computed in the previous section is

$$J_{TN} = \begin{bmatrix} -\beta_1 & 0 & 0 & -\frac{\alpha_1 N \bar{p}_2^{N-1}}{(K_1^N + \bar{p}_2^N)^2} \\ \gamma_1 & -\delta_1 & 0 & 0 \\ 0 & \frac{\alpha_2 N K_2^N \bar{p}_1^{N-1}}{(K_2^N + \bar{p}_1^N)^2} & -\beta_2 & 0 \\ 0 & 0 & \gamma_2 & -\delta_2 \end{bmatrix} \quad (22)$$

and corresponds to the characteristic polynomial

$$\begin{aligned} p_{TN}(s) &= \det(sI - J_{TN}) \\ &= (s + \beta_1)(s + \beta_2)(s + \delta_1)(s + \delta_2) + N^2 \frac{\alpha_1 \alpha_2 \gamma_1 \gamma_2 K_2^N \bar{p}_1^{N-1} \bar{p}_2^{N-1}}{(K_2^N + \bar{p}_1^N)^2 (K_1^N + \bar{p}_2^N)^2}. \end{aligned}$$

In view of the equilibrium conditions in Eq. (20) and Eq. (21), we can write

$$\frac{\alpha_1}{K_1^N + \bar{p}_2^N} = \frac{\beta_1 \delta_1}{\gamma_1} \bar{p}_1 \quad \text{and} \quad \frac{\alpha_2 \bar{p}_1^N}{K_2^N + \bar{p}_1^N} = \frac{\beta_2 \delta_2}{\gamma_2} \bar{p}_2,$$

hence

$$\begin{aligned} N^2 \frac{\alpha_1 \alpha_2 \gamma_1 \gamma_2 K_2^N \bar{p}_1^{N-1} \bar{p}_2^{N-1}}{(K_2^N + \bar{p}_1^N)^2 (K_1^N + \bar{p}_2^N)^2} &= N^2 \gamma_1 \gamma_2 \frac{\alpha_1}{K_1^N + \bar{p}_2^N} \frac{\alpha_2 \bar{p}_1^N}{K_2^N + \bar{p}_1^N} \frac{K_2^N \bar{p}_1^{-1} \bar{p}_2^{N-1}}{(K_2^N + \bar{p}_1^N)(K_1^N + \bar{p}_2^N)} \\ &= N^2 \gamma_1 \gamma_2 \frac{\beta_1 \delta_1}{\gamma_1} \bar{p}_1 \frac{\beta_2 \delta_2}{\gamma_2} \bar{p}_2 \frac{K_2^N \bar{p}_1^{-1} \bar{p}_2^{N-1}}{(K_2^N + \bar{p}_1^N)(K_1^N + \bar{p}_2^N)} = N^2 \beta_1 \beta_2 \delta_1 \delta_2 \frac{K_2^N}{K_2^N + \bar{p}_1^N} \frac{\bar{p}_2^N}{K_1^N + \bar{p}_2^N} \end{aligned}$$

and therefore

$$p_{TN}(s) = (s + \beta_1)(s + \beta_2)(s + \delta_1)(s + \delta_2) + N^2 \beta_1 \beta_2 \delta_1 \delta_2 \frac{K_2^N}{K_2^N + \bar{p}_1^N} \frac{\bar{p}_2^N}{K_1^N + \bar{p}_2^N}.$$

Dividing  $p_{TN}(s)$  by  $\beta_1 \beta_2 \delta_1 \delta_2$ , we can write the characteristic equation as

$$p_{TN}(s) = (1 + s/\beta_1)(1 + s/\beta_2)(1 + s/\delta_1)(1 + s/\delta_2) + N^2 \frac{K_2^N}{K_2^N + \bar{p}_1^N} \frac{\bar{p}_2^N}{K_1^N + \bar{p}_2^N} = 0. \quad (23)$$

**Remark 2** The coefficients  $1/\beta_i$  and  $1/\delta_i$ , for  $i = 1, 2$ , correspond to the time constants  $\tau_i$  in Eq. (3) of the Main Paper, while the term  $N^2 \frac{K_2^N}{K_2^N + \bar{p}_1^N} \frac{\bar{p}_2^N}{K_1^N + \bar{p}_2^N}$  corresponds to the gain  $\kappa$  in Eq. (3) of the Main Paper.

Denoting  $f(\bar{p}_1, \bar{p}_2) = \frac{K_2^N}{K_2^N + \bar{p}_1^N} \frac{\bar{p}_2^N}{K_1^N + \bar{p}_2^N}$ , since  $0 < f(\bar{p}_1, \bar{p}_2) < 1$  and since the closer  $f(\bar{p}_1, \bar{p}_2)$  is to 1, the more likely the system is to oscillate, we can notice that the onset of oscillations is facilitated by small values of  $\bar{p}_1$  and large values of  $\bar{p}_2$ . This is very reasonable, since both decreasing  $\bar{p}_1$  and increasing  $\bar{p}_2$  leads to an increase in the gain value.

### 3.3 Two-node oscillator: conditions for sustained oscillations

In view of Theorem 1, we can state that the minimum value of  $N$  for which the system exhibits sustained oscillations (namely, admits a pair of complex eigenvalues with nonnegative real part, where the eigenvalues are the solution of the characteristic equation (23)) is achieved when  $\beta_1 = \beta_2 = \delta_1 = \delta_2 = b^*$ . Then, the system eigenvalues are the solutions of

$$(1 + s/b^*)^4 + N^2 f(\bar{p}_1, \bar{p}_2) = 0,$$

hence

$$\frac{s}{b^*} = -1 + \sqrt[4]{-1} \sqrt[4]{N^2} \sqrt[4]{f(\bar{p}_1, \bar{p}_2)}.$$

Therefore, since  $f(\bar{p}_1, \bar{p}_2) < 1$ , the critical condition for the system to admit complex eigenvalues with a nonnegative real part is  $\cos(\pi/4)\sqrt[4]{N} > 1$ , hence

$$N > 2. \tag{24}$$

We can now state and prove the following result, which provides a characterisation of the oscillatory region in the parameter space.

**Proposition 5** *The two following conditions are equivalent.*

- (i) *There exists at least one choice of parameters for the two-node oscillator for which the characteristic equation (23) admits complex solutions with a nonnegative real part.*
- (ii) *The inequality (24) is satisfied.*

**Proof** Necessity follows from the same considerations as in the proof of Proposition 4: in view of Theorem 1, the smallest value of the gain required to have oscillations is achieved when all the time constants are equal and, in this case, the dominant roots of the characteristic polynomial (23) can have a nonnegative real part only if the condition (24) is satisfied.

To prove sufficiency, we just need to show that we can select values of the parameters for which

$$f(\bar{p}_1, \bar{p}_2) = \frac{K_2^N}{K_2^N + \bar{p}_1^N} \frac{\bar{p}_2^N}{K_1^N + \bar{p}_2^N}$$

becomes arbitrary close to 1. Hence, for given  $K_1$  and  $K_2$ ,  $\bar{p}_1$  has to be small enough and  $\bar{p}_2$  has to be large enough. From the equilibrium conditions in Eq. (20) and Eq. (21), we see that it is a matter of suitably selecting, for instance,  $\gamma_1$  and  $\gamma_2$  to have  $\bar{p}_1$  as small as desired and  $\bar{p}_2$  as large as desired; indeed, we can fix the pair  $(\bar{p}_1, \bar{p}_2)$  and compute suitable values of  $\gamma_1$  and  $\gamma_2$  for which Eq. (20) and Eq. (21) hold. Then, once the parameters have been suitably chosen, the real part of the two dominant roots can actually cross the imaginary axis if the condition (24) is satisfied. ■

## 4 A case study: the *Neurospora crassa* biological clock

In our analysis we have pointed out that a long negative loop of elements with homogeneous time constants promotes oscillation. However, a long chain is not necessary if the system includes a positive feedback and, indeed, even a two-element chain can be oscillating. In the concluding discussion in the Main Paper, we have proposed an academic example of a two-node negative loop in which one node has a positive self-loop. To emphasize this aspect, we consider now the example of a real oscillator composed of a (necessarily present) negative loop, which is sustained by the co-presence of a positive loop.

The genetic network present in the bread mould *Neurospora crassa*, studied in [13], has been shown to be a successful biological oscillator. Here, we provide some considerations showing that the result proposed in [13] are fully consistent with our analysis.

The system describing the genetic network, presented in [13], corresponds to the equations

$$\begin{aligned}
 \dot{f}_1 &= A(f_g - f_1)w^n - \bar{A}f_1 \\
 \dot{f}_r &= S_3(f_g - f_1) + S_4f_1 - D_3f_r \\
 \dot{f}_p &= L_3f_r - D_6f_p \\
 \dot{w} &= E_2u_p - D_8w - nA(f_g - f_1)w^n + n\bar{A}f_1 - Pwf_p^m \\
 \dot{u}_p &= L_1u_{r_1} - D_4u_p - E_2u_p \\
 \dot{u}_{r_1} &= C_1u_{r_0}f_p - D_7u_{r_1} \\
 \dot{u}_{r_0} &= V_1 - D_1u_{r_0} - C_1u_{r_0}f_p
 \end{aligned}$$

associated with the Jacobian matrix

$$\begin{bmatrix}
 -[Aw^n + \bar{A}] & 0 & 0 & nA(f_g - f_1)w^{n-1} & 0 & 0 & 0 \\
 S_4 - S_3 & -D_3 & 0 & 0 & 0 & 0 & 0 \\
 0 & L_3 & -D_6 & 0 & 0 & 0 & 0 \\
 n[Aw^n + \bar{A}] & 0 & -nPwf_p^{m-1} & -\gamma_4 & E_2 & 0 & 0 \\
 0 & 0 & 0 & 0 & -[D_4 + E_2] & L_1 & 0 \\
 0 & 0 & C_1u_{r_0} & 0 & 0 & -D_7 & C_1f_p \\
 0 & 0 & -C_1u_{r_0} & 0 & 0 & 0 & -(D_1 + C_1f_p)
 \end{bmatrix}$$

where  $\gamma_4 = [D_8 + n^2Aw^{n-1}(f_g - f_1) + Pf_p^m]$ .

By suitably renaming the variables, the Jacobian can be rewritten as

$$J_x = \begin{bmatrix}
 -\gamma_1 & 0 & 0 & \delta_1 & 0 & 0 & 0 \\
 \beta_1 & -\gamma_2 & 0 & 0 & 0 & 0 & 0 \\
 0 & \beta_2 & -\gamma_3 & 0 & 0 & 0 & 0 \\
 \delta_2 & 0 & -\beta_3 & -\gamma_4 & \beta_4 & 0 & 0 \\
 0 & 0 & 0 & 0 & -\gamma_5 & \beta_5 & 0 \\
 0 & 0 & \delta_3 & 0 & 0 & -D_7 & \beta_6 \\
 0 & 0 & -\delta_3 & 0 & 0 & 0 & -(\beta_6 + D_1)
 \end{bmatrix}.$$

The only term that is not sign-definite is  $\beta_1 = S_4 - S_3$ . However, we assume it is positive,  $\beta_1 > 0$ , in view of the numerical values reported in [13, Table 1]:  $S_4 = 8.34$  and  $S_3 = 0.000529$ .

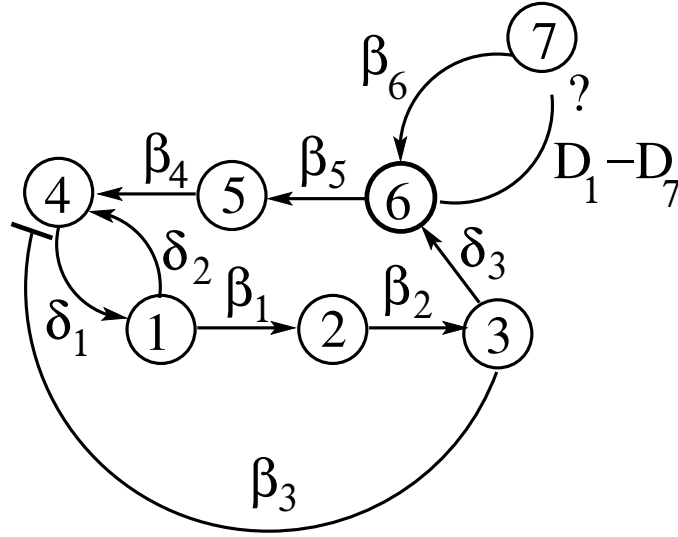


Figure 2: The graph associated with the *Neurospora crassa* system.

The data in [13, Table 2] show that, as the parameter  $D_7$  increases, oscillations are less likely to occur. This can be also shown with our analytic approach. Indeed, if we replace the last variable  $x_7$  by  $\hat{x}_7 = x_7 + x_6$ , the Jacobian becomes

$$\begin{bmatrix} -\gamma_1 & 0 & 0 & \delta_1 & 0 & 0 & 0 \\ \beta_1 & -\gamma_2 & 0 & 0 & 0 & 0 & 0 \\ 0 & \beta_2 & -\gamma_3 & 0 & 0 & 0 & 0 \\ \delta_2 & 0 & -\beta_3 & -\gamma_4 & \beta_4 & 0 & 0 \\ 0 & 0 & 0 & 0 & -\gamma_5 & \beta_5 & 0 \\ 0 & 0 & \delta_3 & 0 & 0 & -(D_7 + \beta_6) & \beta_6 \\ 0 & 0 & 0 & 0 & 0 & D_1 - D_7 & -D_1 \end{bmatrix}.$$

This new Jacobian corresponds to the diagram reported in Figure 2, where the nodes 1-6 correspond to the variables  $x_1-x_6$  and node 7 corresponds to the new variable  $\hat{x}_7$ , while the arcs correspond to the interactions between pairs of nodes (the arc from node  $j$  to node  $i$  is associated with the nonzero  $(i, j)$  entry of the Jacobian matrix). All the arcs are positive, with the exception of the arc from node 3 to 4, associated with the coefficient  $-\beta_3$ , which is negative, and of the arc from node 6 to node 7, associated with the coefficient  $D_1 - D_7$ , which is not sign-definite: it is positive if  $D_1 > D_7$  and negative if  $D_1 < D_7$ .

There are therefore two possible cases.

**Case 1:**  $D_7 < D_1$ . When  $D_7$  is small, hence  $D_1 - D_7 > 0$  is positive, there is a positive feedback from  $\hat{x}_7$  to  $x_6$ , because in this case the arc denoted by a “?” in Figure 2 is positive. If the unique negative off-diagonal entry is set to zero, namely  $\beta_3 = 0$ , the overall system is a monotone system; in fact, the associated Jacobian matrix has exclusively nonnegative off-diagonal entries. The presence of a nonzero entry  $-\beta_3$  introduces a negative loop.

*Negative feedback interconnections of monotone systems* have been deeply investigated in the literature [1] and shown to be typical candidate oscillators [3, 4]. Also in this case, the negative loop created by  $\beta_3$  induces oscillations, as confirmed by the results in [13].

In this case, two loops are present in the system: a negative loop,  $4 \rightarrow 1 \rightarrow 2 \rightarrow 3 \rightarrow 4$ , which is essential for the onset of sustained oscillations (indeed, the presence of a negative loop is necessary for

oscillations [9, 12]), and a positive loop,  $1 \rightarrow 2 \rightarrow 3 \rightarrow 6 \rightarrow 5 \rightarrow 4 \rightarrow 1$ , which has a beneficial effect on the onset of oscillations, since it tends to amplify the effect of the negative one.

**Case 2:**  $D_7 > D_1$ . If  $D_7$  is large,  $D_1 - D_7 < 0$  and the arc denoted by a “?” in Figure 2 is now negative. In this case, two negative loops coexist. The additional negative loop  $z_7 \rightarrow x_6 \dashv z_7$  is short: according to the arguments presented in our paper, short negative loops (as well as loops with one or two dominant time constants) have a strong stabilising effect, because a higher gain is needed to induce sustained oscillations. This is fully consistent with the results reported in [13, Table 2], which show that, for  $D_7$  substantially greater than  $D_1$ , oscillations are less likely to occur: for  $D_7$  large enough, the system becomes arrhythmic.

## References

- [1] D. Angeli and E. D. Sontag, "Oscillations in I/O monotone systems", *IEEE Transactions on Circuits and Systems: Special Issue on Systems Biology* 55 (2008), pp. 166–176.
- [2] F. Blanchini, C. Cuba Samaniego, E. Franco, and G. Giordano, "Design of a molecular clock with RNA-mediated regulation", in *Proceedings of the IEEE Conference on Decision and Control* (2014), pp. 4611–4616.
- [3] F. Blanchini, E. Franco, G. Giordano, "A structural classification of candidate oscillatory and multi-stationary biochemical systems", *Bulletin of Mathematical Biology* 76(10) (2014), pp. 2542–2569.
- [4] F. Blanchini, E. Franco, G. Giordano, "Structural conditions for oscillations and multistationarity in aggregate monotone systems", in *Proceedings of the IEEE Conference on Decision and Control* (2015) pp. 609–614.
- [5] C. Cuba Samaniego, G. Giordano, F. Blanchini, and E. Franco, "Stability analysis of an artificial biomolecular oscillator with non-cooperative regulatory interactions", *Journal of Biological Dynamics* 11(1) (2017), pp. 102-120.
- [6] C. Cuba Samaniego, G. Giordano, J. Kim, F. Blanchini, and E. Franco, "Molecular titration promotes oscillations and bistability in minimal network models with monomeric regulators", *ACS Synthetic Biology* 5 (2016), pp. 321–333.
- [7] C. Cuba Samaniego, S. Kitada, and E. Franco, "Design and analysis of a synthetic aptamer-based oscillator", in *Proceedings of the American Control Conference* (2015), pp. 2655–2660.
- [8] B. C. Goodwin, "Oscillatory behavior in enzymatic control processes", *Advances in Enzyme Regulation* 3 (1965), pp. 425–438.
- [9] J. L. Gouze, "Positive and negative circuits in dynamical systems", *Journal of Biological Systems* 6 (1998), pp. 11–15.
- [10] J. S. Griffith, "Mathematics of cellular control processes. I: Negative feedback to one gene", *Journal of Theoretical Biology* 20(10) (1968), pp. 202–208.
- [11] J. Kim and E. Winfree, "Synthetic *in vitro* transcriptional oscillators", *Molecular Systems Biology*, 7 (2011), pp. 465.
- [12] E. H. Snoussi, "Necessary conditions for multistationarity and stable periodicity", *Journal of Biological Systems* 6 (1998), pp. 3–9.
- [13] Y. Yu, W. Dong, C. Altimus, X. Tang, J. Griffith, M. Morello, L. Dudek, J. Arnold, and H.-B. Schüttler, "A genetic network for the clock of *Neurospora crassa*", *Proceedings of the National Academy of Science* 104(8) (2007) pp. 2809–2814.